buildings

MDPI

Article

Construction and Application of a Multi-Dimensional Quality Gain–Loss Function for Dam Concrete Based on Gaussian Process

Bo Wang [1,2,3], Qikai Li [1], Liang Pei [4], Pengyuan Li [1,5], Hongxiang Li [1], Xiangtian Nie [1,2,3] and Tianyu Fan [1,*]

[1] School of Water Conservancy, North China University of Water Resources and Electric Power, Zhengzhou 450046, China; wangbo@ncwu.edu.cn (B.W.); b202400732@stu.ncwu.edu.cn (Q.L.); x20231010189@stu.ncwu.edu.cn (P.L.); lihongxiang@stu.ncwu.edu.cn (H.L.); niexiangtian@ncwu.edu.cn (X.N.)
[2] Collaborative Innovation Center of Water Resources Efficient Utilization and Support Engineering, Henan Province, Zhengzhou 450046, China
[3] Henan Key Laboratory of Water Environment Simulation and Treatment, Zhengzhou 450046, China
[4] College of Water Conservancy and Hydropower Engineering, Hohai University, Nanjing 210024, China; 241302020016@hhu.edu.cn
[5] Central China Regional Headquarters of Powerchina Road-Bridge Co., Ltd., Zhengzhou 450016, China
* Correspondence: fantianyu@ncwu.edu.cn

Abstract

As a critical component of China's major infrastructure, the quality and safety of hydraulic engineering projects are directly linked to national economic security. Therefore, research on construction quality management of hydraulic concrete is of great importance. Traditional quality gain–loss functions often fail to fully capture the correlations among multiple quality characteristics, the varying weights of these characteristics in overall quality performance, and the presence of multiple influencing factors. To address these limitations, this study employs Gaussian process regression to construct a multivariate and multidimensional quality gain–loss function model. The signal-to-noise ratio is used to represent the interactions among different quality characteristics, while a gain–loss cost matrix is introduced to account for the contribution of each characteristic to the overall function. A case study on summer dam concrete construction is presented to demonstrate the applicability of the proposed model. The results show that the gain–loss values range from a minimum of 1.09 to a maximum of 11.7, which are significantly lower than those obtained using the dimensionless standardized multivariate quality gain–loss function developed by Artiles-León, thereby validating the effectiveness and rationality of the proposed approach.

Keywords: hydropower project management; quality gain–loss function; Gaussian process; quality control; hydraulic concrete; quality compensation

check for updates

Academic Editor: Yasin Onuralp Özkılıç

Received: 28 August 2025
Revised: 29 September 2025
Accepted: 4 October 2025
Published: 24 October 2025

Citation: Wang, B.; Li, Q.; Pei, L.; Li, P.; Li, H.; Nie, X.; Fan, T. Construction and Application of a Multi-Dimensional Quality Gain–Loss Function for Dam Concrete Based on Gaussian Process. *Buildings* **2025**, *15*, 3851. https://doi.org/10.3390/buildings15213851

Copyright: © 2025 by the authors. Licensee MDPI, Basel, Switzerland. This article is an open access article distributed under the terms and conditions of the Creative Commons Attribution (CC BY) license (https://creativecommons.org/licenses/by/4.0/).

1. Introduction

As one of the most critical components of China's major infrastructure, the quality and safety of hydraulic engineering projects are directly related to national economic security. However, due to the combined influence of multiple factors—including raw materials, topography, hydrological conditions, construction techniques, climatic factors, and technical measures—the construction of mass concrete, the primary material in such projects, is often confronted with a series of quality problems such as insufficient strength, air voids, surface defects, and cracking. Therefore, strengthening the management of mass concrete construction and implementing effective quality control throughout the construction process is essential.

Current studies on the quality control of mass or hydraulic concrete mainly focus on mix proportion design [1–3], temperature control [4–9], intelligent monitoring and regulation [10–14], as well as surface inspection and acceptance evaluation. In practical applications, tools such as Pareto charts are often used to identify key issues, histograms are applied to assess and predict product quality, and cause-and-effect diagrams are employed to analyze potential causal relationships [15]. Despite these efforts, research on new theories and innovative methods for quality control in mass concrete construction remains relatively limited.

The concept of the quality loss function was first proposed by Dr. Taguchi in the 1970s, who argued that fluctuations in product quality are inevitable and that any deviation of quality characteristics from their target values results in losses. Since then, scholars worldwide have conducted extensive studies on modeling quality loss, leading to the development of a wide variety of improved models, including fuzzy quality gain–loss functions [16], piecewise loss functions [17–19], inverse normal loss functions [20], and other extensions [21,22]. In the field of multivariate quality gain–loss functions, significant progress has been made: Pignatiello [23] proposed a multi-parameter loss function method based on minimizing deviations from design targets and maximizing robustness; Artiles-León [24] developed a dimensionless "standardized" multivariate loss function; Lee and Tang [25] introduced a total loss function model for multiple correlated quality characteristics, along with its tolerance design method. In addition, domestic and international scholars have proposed a range of optimization approaches combining genetic algorithms, Taguchi methods, and response surface methodology with multivariate quality loss models [26–29].

The conventional quality loss function assumes that the minimum loss occurs when the quality characteristic value equals the target value, with the loss being zero at that point. However, in real construction processes, not only losses but also compensatory effects exist. For example, in mass hydraulic concrete construction, quality control measures can be implemented across all stages—from production to curing—thereby offsetting part of the losses, a phenomenon referred to as quality compensation. To address this limitation, Wang et al. [30–35] redefined the constant term in the Taylor expansion as quality compensation and introduced the concept of the quality gain–loss function. Based on this, they further developed several extended models, such as gain–loss functions for "larger-the-better" and "smaller-the-better" characteristics, fuzzy gain–loss functions, grey gain–loss functions, quadratic exponential functions, and multivariate gain–loss functions. Nevertheless, existing research has not adequately accounted for correlations among multiple quality characteristics, the weight of each characteristic in overall gain–loss, or the presence of multiple influencing factors.

Gaussian process (GP) modeling, developed from Gaussian stochastic processes, kernel methods, and Bayesian inference, is a machine learning approach particularly well-suited to handling high-dimensional, small-sample, and nonlinear problems. It has been widely applied to modeling complex nonlinear input–output relationships and has gradually gained attention in civil and hydraulic engineering in recent years. For instance, Zhang et al. [36] developed a GP-based model to predict the strength of high-performance concrete; Luo [37] proposed a GP-based dam deformation prediction model; Zhai et al. [38] combined GP with multivariate quality loss functions to design robust parameters under high-dimensional experimental data; Liu et al. [39] improved multi-output GP regression for compaction characteristics of earth–rockfill dams; and several other researchers have successfully applied GP to predict hydrological series, reservoir runoff, dam settlement, mechanical parameter inversion, and deformation behavior [40–46].

Building upon quality gain–loss theory, this study integrates the signal-to-noise ratio with the Gaussian process framework and proposes a multivariate and multidimensional quality gain–loss function model based on Gaussian processes. The model aims to address the correlations among multiple quality characteristics and improve the accuracy and applicability of quality control in mass hydraulic concrete construction.

2. Multivariate Quality Gain–Loss Function Based on Artiles-León

Artiles-León constructs a dimensionless "standardized" multivariate QLF $L_A(y_1, y_2, \cdots y_n)$ [9] to make the QLF independent of the unit.

$$L_A(y_1, y_2, \cdots y_n) = 4\sum_{i=1}^{n}\left(\frac{y_i - T_i}{T_U^i - T_L^i}\right)^2 \tag{1}$$

where T_i, T_U^i and T_L^i are the target value and upper and lower specification limits of quality characteristic y_i, respectively.

Considering the quality compensation term, the corresponding multiple quality gain–loss function $G_A(y_1, y_2, \cdots y_n)$ is defined as follows:

$$G_A(y_1, y_2, \cdots y_n) = 4\sum_{i=1}^{n}\left(\frac{y_i - T_i}{T_U^i - T_L^i}\right)^2 + \sum_{i=1}^{n} g(y_i) \tag{2}$$

where $g(y_i)$ is the compensation function of the quality characteristic y_i.

3. Traditional Multivariate Quality Gain–Loss Function

Conventional quality loss theory posits that product quality loss is determined using a multivariate functional relationship with its quality characteristics and proposes a multivariate QLF for the quantitative analysis of multiple quality characteristics $L_C(q_1, q_2, \cdots, q_h, \cdots, q_I)$ as follows [8]:

$$L_C(q_1, q_2, \cdots, q_h, \cdots, q_I) = f(q_1, q_2, \cdots, q_h, \cdots, q_I) \tag{3}$$

In the neighborhood D, if a function of several variables has three consecutive partial derivatives at its origin P_0 (0, 0, 0), and then $L_C(q_1, q_2, \cdots, q_h, \cdots, q_I)$ is defined as follows:

$$\begin{aligned} &L_C(q_1, q_2, \cdots, q_h, \cdots, q_I) = f(q_1, q_2, \cdots, q_h, \cdots, q_I) \\ &= f(0, 0, \cdots, 0) + \sum_{h=1}^{I} f'_{q_h}(0, 0, \cdots, 0) q_h \\ &+ \frac{1}{2!}\sum_{h_1=1, h_2=1}^{I} f''_{q_{h_1} q_{h_2}}(0, 0, \cdots, 0) q_{h_1} q_{h_2} \\ &+ \frac{1}{3!}\sum_{h_1, h_2, h_3=1}^{I} f'''_{q_{h_1} q_{h_2} q_{h_3}}(\theta q_1, \theta q_2, \cdots, \theta q_h, \cdots, \theta q_I) \end{aligned} \tag{4}$$

where $q_1, q_2, \cdots, q_h, \cdots, q_I$ are I quality characteristics. When $q_1, q_2, \cdots, q_h, \cdots, q_I = 0$, there is a minimum quality loss, $f'_{q_h}(0, 0, \cdots, 0) = 0$, for $h = 1, 2, \cdots, I$, with $0 < \theta < 1$.

When defining $f(0, 0, \cdots, 0) = E \in R$ as the quality compensation component and neglecting higher-order terms beyond the quadratic order, the corresponding multivariate quality gain–loss function $G_C(q_1, q_2, \cdots, q_h, \cdots, q_I)$ is formulated as follows:

$$\begin{aligned} G_C(q_1, q_2, \cdots, q_h, \cdots, q_I) &= E + \tfrac{1}{2!}\sum_{h_1=1, h_2=1}^{I} f''_{q_{h_1} q_{h_2}}(0, 0, \cdots, 0) q_{h_1} q_{h_2} \\ &= E + \sum_{i=1}^{I} k_{ii} q_i^2 + \sum_{i=1, i<j}^{I} k_{ij} q_i q_j \end{aligned} \tag{5}$$

where E is the maximum quality compensation, k_{ii} is the self-influencing item q_{ii}^2 quality loss weight, and k_{ij} ($i < j$) is the mutual influence term $q_i q_j$ quality loss weight. Considering that the compensation quantity in engineering practice is not always constant, the quality compensation function $E(q_1, q_2, \cdots, q_h, \cdots, q_I)$ is defined as follows:

$$E(q_1, q_2, \cdots, q_h, \cdots, q_I) = g(q_1, q_2, \cdots, q_h, \cdots, q_I) \tag{6}$$

Then, the multivariate quality gain–loss function $G_C(q_1, q_2, \cdots, q_h, \cdots, q_I)$ is defined as follows:

$$\begin{aligned} &G_C(q_1, q_2, \cdots, q_h, \cdots, q_I) = g(q_1, q_2, \cdots, q_h, \cdots, q_I) \\ &+\tfrac{1}{2!}\sum_{h_1=1,h_2=1}^{I} f''_{q_{h_1}q_{h_2}}(0, 0, \cdots, 0) q_{h_1} q_{h_2} \\ &= g(q_1, q_2, \cdots, q_h, \cdots, q_I) + \sum_{i=1}^{I} k_{ii} q_i^2 + \sum_{i=1, i<j}^{I} k_{ij} q_i q_j \\ &= \sum_{i=1}^{I} [k_{ii} q_i^2 + g_i(q_i)] + \sum_{i=1, i<j}^{I} (k_{ij} + e_{ij}) q_i q_j \\ &= \sum_{i=1}^{I} [k_{ii} q_i^2 + g_i(q_i)] + \sum_{i=1, i<j}^{I} \omega_{ij} q_i q_j \end{aligned} \tag{7}$$

where e_{ij} is the mutual influence term of the quality compensation weight $q_i q_j$; ω_{ij} is the mutual influence term of the quality gain and loss weight $q_i q_j$; $g_i(q_i)$ is the quality compensation function of the quality index q_i.

For an arbitrary i (i = 1, 2, …, I), when all $q_k = 0$ ($k \neq I$) are considered, ζ_i is the tolerance of the quality characteristic q_i, and A_i is the quality gain or loss corresponding to q_i, then the quality loss coefficient k_{ii} of the self-influencing term is defined as follows:

$$k_{ii} = [A_i - g_i(\zeta_i)]/\zeta_i^2 \tag{8}$$

For any i, j (i, j = 1, 2, …, I, $i < j$), when all $q_k = 0$ ($k \neq i, k \neq j$) are considered, ζ_{ij}^i is the ij interaction tolerance of the quality characteristic i, ζ_{ij}^j is the ij interaction tolerance of the quality characteristic j, and A_{ij} is the interaction quality gain or loss, then,

$$\omega_{ij} = \frac{A_{ij} - [k_{ii}(\zeta_{ij}^i)^2 + g_i(\zeta_{ij}^i)] - [k_{jj}(\zeta_{ij}^j)^2 + g_i(\zeta_{ij}^j)]}{\zeta_{ij}^i \zeta_{ij}^j} \tag{9}$$

4. Multi-Dimensional Quality Gain–Loss Function Based on Gaussian Process

4.1. Principle of GPR Model

Let X be the input space, where x ∈ X is a K-dimensional input factor and $f(x)$ is the corresponding output response. Then,

$$f(x) \sim GP(m(x), k(x, x')) \tag{10}$$

Herein, $m(x)$ denotes the mean function while $k(x, x')$ represents the covariance function in the formulation; $f(x)$ is the potential function, $y(x)$ is the observation function, $y(x) = f(x) + \varepsilon$, and ε is the noise vector. The Gaussian prior distribution characteristics of $y(x)$ are determined by the mean vector μ and the covariance matrix Σ. In the absence of prior knowledge regarding the expected value of $y(x)$ before acquiring observational data, the mean vector is conventionally set to zero in the formulation.

In the proposed formulation, the covariance kernel is represented as a kernel function incorporating the standard Gaussian noise term σ_n^2, which quantifies the pairwise similarity relationships within the observed dataset.

$$\mathrm{cov}(y(x_p), y(x_q)) = k(x_p, x_q) + \sigma_n^2 \delta_{pq} \tag{11}$$

where δ_{pq} is the Kronecker symbolic function; when p = q, $\delta_{pq} = 1$, otherwise, it is 0.

$$k_{SE}(x_i, x_j) = \sigma_f^2 \exp\left(-\frac{1}{2l^2}\left\|x_i - x_j\right\|^2\right) \tag{12}$$

where k_{SE} is the squared exceptional covariance function; $x_i = (x_{i1}, x_{i2}, \ldots, x_{ik})$ and $x_j = (x_{j1}, x_{j2}, \ldots, x_{jk})$; σ_f^2 is the signal variance, which is used to adjust the covariance function; l is the length scale. For uncorrelated inputs, l is maximized, at which time the exponential term approaches 1, so that the covariance function value is basically independent of the input, and the uncorrelated inputs are effectively removed.

The hyperparameter $\theta = [l, \sigma_f, \sigma_n]^T$ is optimized using the maximum edge likelihood method. The steps are as follows:

Step 1: Establish the edge likelihood function of the training sample set $p(y|X, \theta)$ as follows:

$$p(y\Big|X, \theta) \sim N(0, K + \sigma_n^2 I) \tag{13}$$

Step 2: Build the negative log-edge likelihood function $-\log p(y|X, \theta)$ as follows:

$$-\log p(y|X, \theta) = \tfrac{1}{2} y^T G^{-1} y + \tfrac{1}{2} \log|G| + \tfrac{n}{2} \log 2\pi \tag{14}$$

and

$$G = K + \sigma_n^2 I \tag{15}$$

Step 3: Following unconstrained optimization principles, the hyperparameter tuning process minimizes the negative log-marginal likelihood function as its objective criterion. The conjugate gradient method is then utilized to determine the optimal hyperparameter. In the context of the squared exponential covariance kernel, the gradient of the log-marginal likelihood function with respect to each hyperparameter can be analytically formulated as follows:

$$\frac{\partial \log p(y|X, \theta)}{\partial l} = -\frac{1}{2} y^T G^{-1} \frac{\partial G}{\partial l} G^{-1} y - \frac{1}{2} tr\left(G^{-1} \frac{\partial G}{\partial l}\right) \tag{16}$$

$$\frac{\partial \log p(y|X, \theta)}{\partial \sigma_f} = -\tfrac{1}{2} y^T G^{-1} \tfrac{\partial G}{\partial \sigma_f} G^{-1} y - \tfrac{1}{2} tr\left(G^{-1} \tfrac{\partial G}{\partial \sigma_f}\right) \tag{17}$$

and

$$\frac{\partial \log p(y|X, \theta)}{\partial \sigma_n} = -\frac{1}{2} y^T G^{-1} \frac{\partial G}{\partial \sigma_n} G^{-1} y - \frac{1}{2} tr\left(G^{-1} \frac{\partial G}{\partial \sigma_n}\right) \tag{18}$$

In this context, $tr(\cdot)$ quantifies the matrix trace operation, which mathematically corresponds to the aggregation of all diagonal elements positioned along the principal diagonal axis of the square matrix structure.

Let the potential function f be formed using n training sample points set X, and let the potential function f_* be formed using m test sample points set X_*. The joint prior distribution of f and f_* is defined as follows:

$$\begin{bmatrix} f \\ f_* \end{bmatrix} \sim N\left(0, \begin{bmatrix} K & K_*^T \\ K_* & K_{**} \end{bmatrix}\right) \tag{19}$$

where K_*, K_{**}, and K are covariance matrices, defined as follows:

$$K = K(X, X) = \begin{bmatrix} k(x_1, x_1) & k(x_1, x_2) & \cdots & k(x_1, x_n) \\ k(x_2, x_1) & k(x_2, x_2) & \cdots & k(x_2, x_n) \\ \vdots & \vdots & \ddots & \vdots \\ k(x_n, x_1) & k(x_n, x_2) & \cdots & k(x_n, x_n) \end{bmatrix} \tag{20}$$

$$K_* = K(X_*, X) = \begin{bmatrix} k(x_*^{(1)}, x_1) & k(x_*^{(1)}, x_2) & \cdots & k(x_*^{(1)}, x_n) \\ k(x_*^{(2)}, x_1) & k(x_*^{(2)}, x_2) & \cdots & k(x_*^{(2)}, x_n) \\ \vdots & \vdots & \ddots & \vdots \\ k(x_*^{(n)}, x_1) & k(x_*^{(n)}, x_2) & \cdots & k(x_*^{(n)}, x_n) \end{bmatrix} \text{and} \tag{21}$$

$$K_{**} = K(X_*, X_*) = \begin{bmatrix} k(x_*^{(1)}, x_*^{(1)}) & k(x_*^{(1)}, x_*^{(2)}) & \cdots & k(x_*^{(1)}, x_*^{(n)}) \\ k(x_*^{(2)}, x_*^{(1)}) & k(x_*^{(2)}, x_*^{(2)}) & \cdots & k(x_*^{(2)}, x_*^{(n)}) \\ \vdots & \vdots & \ddots & \vdots \\ k(x_*^{(n)}, x_*^{(1)}) & k(x_*^{(n)}, x_*^{(2)}) & \cdots & k(x_*^{(n)}, x_*^{(n)}) \end{bmatrix} \tag{22}$$

Assuming that the noise distribution satisfies an independent and homogeneous Gaussian distribution, $\varepsilon \sim N(0, \sigma_n^2)$, the joint prior distribution of y and f_* is defined as follows:

$$\begin{bmatrix} y \\ f_* \end{bmatrix} \sim N\left(0, \begin{bmatrix} K + \sigma_n^2 \mathrm{I} & K_*^{\mathrm{T}} \\ K_* & K_{**} \end{bmatrix}\right) \tag{23}$$

The posterior distribution of f_* is defined as follows:

$$f_* | y \sim N\left(K_*[K + \sigma_n^2 I]^{-1} y, K_{**} - K_*[K + \sigma_n^2 I]^{-1} K_*^T\right) \tag{24}$$

Let $\overline{f_*}$ be the mean of the predicted distribution and σ_*^2 be the variance of the predicted distribution, then

$$\overline{f_*} = K_*[K + \sigma_n^2 I]^{-1} y \text{and} \tag{25}$$

$$\sigma_*^2 = K_{**} - K_*[K + \sigma_n^2 I]^{-1} K_*^T \tag{26}$$

4.2. Signal-to-Noise Ratio (SNR)

The quality characteristic value of a product is a random variable under the action of many factors. Assume that the mathematical expected value is μ and the variance is σ^2. For a nominal-the-type characteristic, the closer μ is to the target value T, the better, and the smaller σ^2 is, the better. In robust design, let the difference coefficient be γ and the SNR be η, then

$$\gamma = \frac{\sigma}{\mu} \text{and} \tag{27}$$

$$\eta = \frac{\mu^2}{\sigma^2} \tag{28}$$

The signal-to-noise ratio of the nominal-the-type characteristic η_T is given as follows:

$$\eta_T = 10 \log \frac{\mu^2}{\sigma^2} \tag{29}$$

Let $\overline{y} = \frac{1}{n}\sum_{i=1}^{n} y_i$ and $S^2 = \frac{1}{n-1}\sum_{i=1}^{n}(y_i - \overline{y})^2$, then the estimated value $\hat{\eta_T}$ of η_T is defined as follows:

$$\hat{\eta_T} = 10\log\left(\frac{\overline{y}^2}{S^2}\right) \tag{30}$$

Similarly, the signal-to-noise ratio for a larger-the-better characteristic η_L and its estimated value $\hat{\eta_T}$ are given as follows:

$$\eta_L = 10\log\left(\sigma^2 + \mu^2\right) \text{and} \tag{31}$$

$$\hat{\eta_L} = -10\log\left(\frac{1}{n}\sum_{i=1}^{n}\frac{1}{{y_i}^2}\right) \tag{32}$$

The signal-to-noise ratio for a smaller-the-better type characteristic η_S and its estimated value $\hat{\eta_S}$ are defined as follows:

$$\eta_S = 10\log\frac{1}{\mu^2 + \sigma^2} \text{and} \tag{33}$$

$$\hat{\eta_S} = -10\log\left(\frac{1}{n}\sum_{i=1}^{n}{y_i}^2\right) \tag{34}$$

The signal-to-noise ratio is a monotone function of the variation coefficient γ, which is an important index reflecting the stability of product quality. The stability of the product is positively correlated with the coefficient of η. When the value of η increases, the quality loss is significantly reduced.

The variation coefficient γ and the signal-to-noise ratio η are dimensionless data, and both consider the influence of mean value and variance on quality stability. However, η is close to the normal distribution, which makes the quality characteristics linearly additive, so interactions can be ignored.

4.3. Multi-Dimensional Quality Gain–Loss Function Based on Gaussian Process

The gain and loss weight λ_i of the quality characteristic y_i is given as follows:

$$\lambda_i = \frac{\frac{1}{\eta_i}}{\sum_{j=1}^{p}\frac{1}{\eta_j}} \tag{35}$$

Construct the weight matrix $C = (\lambda_1, \lambda_2, \cdots \lambda_p)^{\mathrm{T}}$ and the gain–loss cost matrix $C_1 = diag(\lambda_1, \lambda_2, \cdots \lambda_p)$ from the gain and loss weights. The multi-dimensional quality gain–loss functions $G_{GL}(y(x))$, $G_{GS}(y(x))$, and $G_{GT}(y(x))$ for the quality characteristics of the larger-the-better, smaller-the-better, and nominal-the-best type are defined as follows:

$$G_{GL}(y(x)) = \begin{bmatrix} k_1(y_1(x))^{-1} \\ k_2(y_2(x))^{-1} \\ \vdots \\ k_p(y_p(x))^{-1} \end{bmatrix}^T \begin{bmatrix} \lambda_1 & 0 & \cdots & 0 \\ 0 & \lambda_2 & \cdots & 0 \\ \vdots & \vdots & \ddots & \vdots \\ 0 & 0 & \cdots & \lambda_p \end{bmatrix} \begin{bmatrix} (y_1(x))^{-1} \\ (y_2(x))^{-1} \\ \vdots \\ (y_p(x))^{-1} \end{bmatrix} + \begin{bmatrix} g((y_1(x))^{-1}) \\ g((y_2(x))^{-1}) \\ \vdots \\ g((y_p(x))^{-1}) \end{bmatrix}^T \begin{bmatrix} \lambda_1 \\ \lambda_2 \\ \vdots \\ \lambda_p \end{bmatrix} = \sum_{i=1}^{p} \lambda_i[k_i((y_i(x))^{-1})^2 + g((y_i(x))^{-1})] \tag{36}$$

$$G_{GS}(y(x)) = \begin{bmatrix} k_1 y_1(x) \\ k_2 y_2(x) \\ \vdots \\ k_p y_p(x) \end{bmatrix}^T \begin{bmatrix} \lambda_1 & 0 & \cdots & 0 \\ 0 & \lambda_2 & \cdots & 0 \\ \vdots & \vdots & \ddots & \vdots \\ 0 & 0 & \cdots & \lambda_p \end{bmatrix} \begin{bmatrix} y_1(x) \\ y_2(x) \\ \vdots \\ y_p(x) \end{bmatrix} + \begin{bmatrix} g(y_1(x)) \\ g(y_2(x)) \\ \vdots \\ g(y_p(x)) \end{bmatrix}^T \begin{bmatrix} \lambda_1 \\ \lambda_2 \\ \vdots \\ \lambda_p \end{bmatrix} = \sum_{i=1}^{p} \lambda_i [k_i (y_i(x))^2 + g(y_i(x))] \quad (37)$$

and

$$G_{GT}(y(x)) = \begin{bmatrix} k_1 y_1(x) - T_1 \\ k_2 y_2(x) - T_2 \\ \vdots \\ k_p y_p(x) - T_p \end{bmatrix}^T \begin{bmatrix} \lambda_1 & 0 & \cdots & 0 \\ 0 & \lambda_2 & \cdots & 0 \\ \vdots & \vdots & \ddots & \vdots \\ 0 & 0 & \cdots & \lambda_p \end{bmatrix} \begin{bmatrix} y_1(x) - T_1 \\ y_2(x) - T_2 \\ \vdots \\ y_p(x) - T_p \end{bmatrix} + \begin{bmatrix} g(y_1(x) - T_1) \\ g(y_2(x) - T_2) \\ \vdots \\ g(y_p(x) - T_p) \end{bmatrix}^T \begin{bmatrix} \lambda_1 \\ \lambda_2 \\ \vdots \\ \lambda_p \end{bmatrix} = \sum_{i=1}^{p} \lambda_i [k_i (y_i(x) - T_i)^2 + g(y_i(x) - T_i)] \quad (38)$$

Let

$$G(y_i(x)) = \begin{cases} k_i (y_i(x) - T_i)^2 + g(y_i(x) - T_i) \\ k_i ((y_i(x))^{-1})^2 + g((y_i(x))^{-1}) \\ k_i (y_i(x))^2 + g(y_i(x)) \end{cases} \quad (39)$$

Then, Equations (36)–(38) can be unified into the following forms:

$$G(y(x)) = \sum_{i=1}^{p} \lambda_i G(y_i(x)) \quad (40)$$

where $G(y_i(x))$ is the quality gain–loss function of the quality characteristic y_i.

Within the GPR modeling paradigm, this study synthesizes a novel multi-dimensional quality assessment framework by integrating the proposed gain–loss function architecture. A multi-dimensional quality gain–loss function model based on GPR is then constructed as follows:

$$G(y(x)) = \sum_{i=1}^{p} \lambda_i G(y_i(x)) \quad (41)$$

The construction flowchart of the multi-dimensional quality gain–loss function model, combined with GPR and SNR, is shown in Figure 1.

The specific steps are as follows:

Step 1: Collect multidimensional test data and perform normalization. Use the test data to construct the initial GPR model while selecting the optimization algorithm, kernel function type, and initial parameters.

Step 2: Utilize the optimization algorithm to approximate the simulation of hyperparameters based on the training and test data. Predict the training and test sets, then reverse-normalize the predicted results and compare them with the original data.

Step 3: Calculate performance metrics, such as Root Mean Square Error (RMSE), Coefficient of Determination (R^2), Mean Squared Error (MSE), Residual Prediction Deviation, Mean Absolute Error (MAE), and Mean Absolute Percentage Error (MAPE), to evaluate the prediction accuracy of the model, and finalize the GPR model.

Step 4: Use the GPR model to establish the predictive relationship between impact factors and quality characteristics. Based on the model's characteristics, compute the signal-to-noise ratio (SNR) to determine the gain–loss weight of each quality characteristic.

Step 5: Generate the gain–loss cost matrix using the computed gain–loss weights and construct the multidimensional quality gain–loss function.

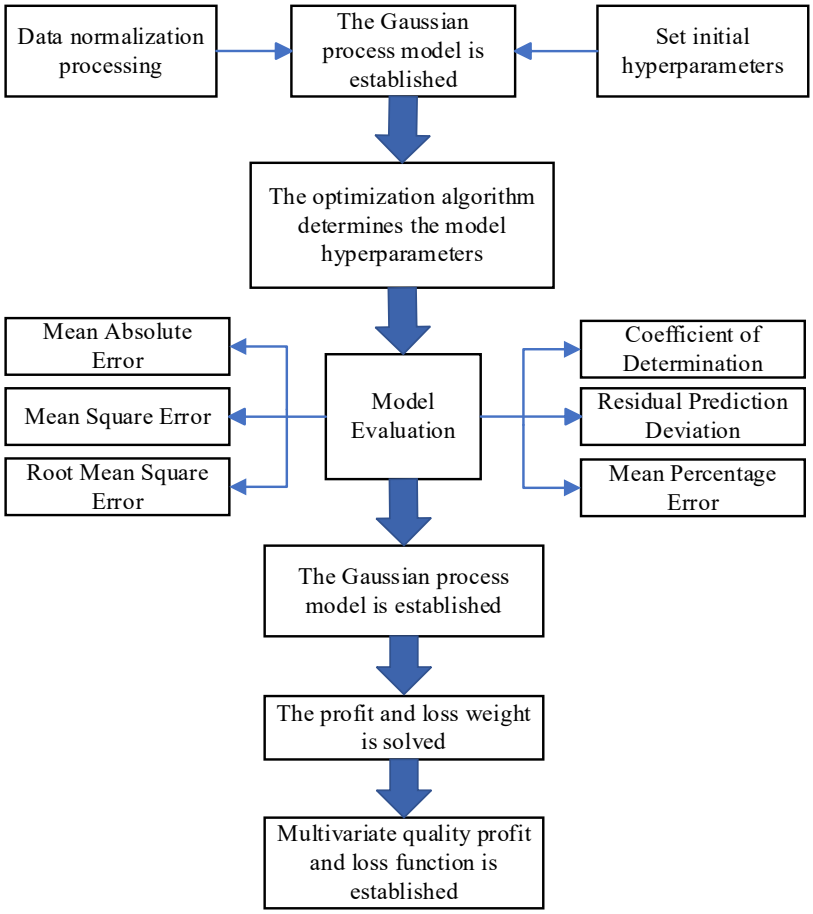


Figure 1. Construction flowchart of the multi-dimensional quality gain–loss function model combining the Gaussian process and SNR.

5. Case Analysis

5.1. Project Overview

During the high-temperature season, dam concrete construction utilizes a tower conveyor system for both horizontal and vertical transport, which shortens warehousing time and enhances production efficiency. The horizontal concrete transport system consists of five to seven belts, covering distances of 400 to 800 m. Due to the dispersion of concrete along the feeding line and multiple turnovers, the concrete is significantly influenced by external temperatures. As the concrete moves along the thin layer of the conveyor belt, some of the aggregate gradually floats to the surface, leading to a loss of concrete mortar and slump. To mitigate the temperature rise of the concrete, the temperature rise rate of the pre-cooled concrete from the exit to the warehouse surface should not exceed 0.25 during the high-temperature season. Additionally, to counteract the loss of concrete mortar and slump, mortar loss should be controlled within 1.5%, and the slump should be maintained within 4 cm.

There are numerous factors that influence the quality of concrete. Since existing research primarily focuses on temperature control in mass concrete, this study assumes that parameters such as viscosity and yield strength remain constant. Instead, the emphasis is placed on three key quality characteristics—temperature rise rate $y_1(x_i)$, mortar loss rate y_2, and slump y_3—for which the corresponding quality gain–loss values are calculated. The three primary quality characteristics in dam concrete construction—temperature recovery rate $y_1(x_i)$, mortar loss rate y_2, and slump degree y_3—are influenced by several factors. Specifically, the influencing factors for the temperature recovery rate $y_1(x_i)$ include concrete

loading speed x_1, silo surface exposure time x_2, and exit temperature x_3. The temperature recovery rate $y_1(x_i)$ and mortar loss rate y_2 are classified as low-quality characteristics, while the slump degree y_3 is an expected quality characteristic, with a target value of 4 cm.

5.2. Multi-Dimensional Quality Gain–Loss Function Based on Gaussian Process Analyze

5.2.1. Construction of Gaussian Process Regression Model

A dataset comprising 100 training instances and 30 testing cases was utilized to quantify warehousing operational velocity, warehouse surface exposure time, exit temperature, and temperature recovery rate. The GPR model was constructed using MATLAB R2022a, with the squared exponential covariance function selected as the kernel function and initial hyperparameters chosen accordingly. The optimal hyperparameters were determined based on the training data. The prediction results were obtained by substituting the test samples into the model. To assess the model's predictive capability, several metrics were calculated, including Root Mean Square Error (RMSE), Coefficient of Determination (R^2), Mean Squared Error (MSE), Residual Prediction Deviation (RPD), Mean Absolute Error (MAE), and Mean Absolute Percentage Error (MAPE). The evaluation results of the GPR model are presented in Table 1.

Table 1. Model evaluation results table.

Evaluation Index	RMSE	R^2	MSE	RPD	MAE	MAPE
Evaluation result	0.026716	0.96074	0.00071375	5.9686	0.018491	0.068282

Smaller values of Root Mean Square Error (RMSE), Mean Square Error (MSE), Mean Absolute Error (MAE), and Mean Absolute Percentage Error (MAPE) indicate better model performance, with the Coefficient of Determination (R^2) approaching 1. Conversely, a larger Residual Prediction Deviation (RPD) suggests smaller prediction errors and a higher degree of model fit. As shown in Table 1, the model exhibits strong predictive performance, and the prediction results for the temperature recovery rate are presented in Table 2.

Table 2. Forecast results of the temperature recovery rate.

Serial Number	1	2	3	4	5	6	7	8	9	10
x_1 (m^3/h)	130	130	130	128	126	125	125	123	120	120
x_2 (h)	3	3	4	3	3	3	3.5	4	4	4
x_3 (°C)	8	10	10	7	9	10	8	7	7	8
y_1 (x_i)	0.12	0.18	0.22	0.10	0.15	0.18	0.11	0.17	0.18	0.20

5.2.2. Construction of Multi-Dimensional Quality Gain–Loss Function

The temperature recovery rate $y_1(x_i)$ was calculated according to the mortar loss rate y_2, the collapse degree y_3, and the GPR model. Table 3 lists the sample data.

Table 3. Sample data table.

Group	1	2	3	4	5	6	7	8	9	10
y_1 (x_i)	0.12	0.18	0.22	0.10	0.15	0.18	0.11	0.17	0.18	0.20
y_2 (%)	1	0.5	1	1.5	0.5	0.5	1	1	0.5	1
y_3 (cm)	3	4	6	4	2	3	5	3	6	4

According to the sample data in Table 3, the SNR of temperature recovery rate, mortar loss rate, and collapse degree are $\eta_1 = 15.63$, $\eta_2 = 40.84$, and $\eta_3 = 9$, respectively. The

gain–loss weights are $\lambda_1 = 32.0\%$, $\lambda_2 = 12.3\%$, and $\lambda_3 = 55.7\%$, respectively. Because $\lambda_3 > \lambda_1 > \lambda_2$, the "contribution" of collapse degree to quality gain–loss is the largest among the three quality characteristics. The weight matrix $C = (0.320, 0.123, 0.557)^T$ and gain–loss cost matrix $C_1 = diag(0.320, 0.123, 0.557)$ are obtained from the gain–loss weights. The multi-dimensional quality gain–loss function is given as follows:

$$G(y(x)) = \begin{bmatrix} k_1 y_1(x) \\ k_2 y_2 \\ k_3(y_3 - T) \end{bmatrix}^T \begin{bmatrix} \lambda_1 & 0 & 0 \\ 0 & \lambda_2 & 0 \\ 0 & 0 & \lambda_3 \end{bmatrix} \begin{bmatrix} y_1(x) \\ y_2 \\ y_3 - T \end{bmatrix} + \begin{bmatrix} g(y_1(x)) \\ g(y_2) \\ g(y_3 - T) \end{bmatrix}^T \begin{bmatrix} \lambda_1 \\ \lambda_2 \\ \lambda_3 \end{bmatrix} = 0.320\left[k_1 y_1(x)^2 + g(y_1(x))\right] + 0.123\left[k_2 y_2^2 + g(y_2)\right] + 0.557\left[k_3(y_3 - 4)^2 + g(y_3 - 4)\right].$$

5.3. Multi-Dimensional Quality Gain–Loss Calculation and Comparative Analysis

5.3.1. Multi-Dimensional Quality Gain–Loss Calculation

When $y_1(x_i) = y_2 = 0$ and the collapse is less than 2 cm, the concrete pouring workability is not up to standard. When the collapse is greater than 6 cm, the aggregate tends to segregate during transportation, leading to a decrease in concrete strength. The quality loss is 24 yuan/m^3, and the compensation amount for the collapse loss is 3 yuan/m^3. The final quality gain–loss is 11 yuan/m^3 due to the mutual influence of quality characteristics. When $y_2 = 0$, $y_3 = 4$, and $y_1(x_i) = 0.25$, the surface and internal cracks of concrete are too large, the quality loss is 24 yuan/m^3, the compensation amount is 2.4 yuan/m^3, and the quality gain–loss is 5.2 yuan/m^3. When $y_1(x_i) = 0$, $y_3 = 4$, and $y_2 = 0.015$, the quality loss is 24 yuan/m^3, the compensation amount is $640y_2$ yuan/m^3, and the quality gain–loss is -0.7 yuan/m^3.

When $y_3 = 4$, $y_1(x_i) = 0.25$, and $y_2 = 0.015$, both the temperature recovery rate and the mortar loss rate reach the tolerance limit, and the quality gain–loss is 10 yuan/m^3. When $y_2 = 0$, $y_1(x_i) = 0.25$, and $y_3 = 2$, the temperature recovery rate and collapse reach the tolerance limit, and the quality gain–loss is 18.5 yuan/m^3. When $y_1(x_i) = 0$, $y_2 = 0.015$, and $y_3 = 2$, the loss rate and collapse of mortar reach the tolerance limit, and the quality gain–loss is 15 yuan/m^3. Table 4 lists the function conditions.

Table 4. Function conditions table.

Conditions	Condition 1	Condition 2	Condition 3	Condition 4	Condition 5	Condition 6
y_1 (x_i)	0	0	0.25	0	0.25	0.25
y_2 (%)	0	0.015	0	0.015	0	0.015
y_3 (cm)	2	4	4	2	2	4
Compensating quantity (yuan/m^3)	-3	$-640y_2$	-2.4	/	/	/
Gain–loss value (yuan/m^3)	11	-0.7	5.2	11	18.5	12.5

Model 1 Multiple quality gain–loss calculations based on Artiles-León

According to conditions 1, 2, and 3 in Table 4, the multiple quality gain–loss function based on Artiles-León can be obtained as follows:

$$L(y_1, y_2, y_3) = 4[2.65(\tfrac{y_1(x)}{0.25})^2 + 3.575(\tfrac{y_2}{0.015})^2 + 16.4(\tfrac{y_3 - 4}{4})^2] - 2.4 - 640y_2 - 3 \quad (42)$$

Model 2 Traditional multivariate quality gain–loss calculation

According to conditions 1–6 in Table 4, the traditional multivariate quality gain–loss function is expressed as follows:

$$Q = 271.36y_1^2 - 2.4 + 63555.5y_2^2 - 640y_2 + 4.1(y_3 - 4)^2 - 3 \\ -106.67y_1y_2 + 6.2y_1(y_3 - 4) + 236.67y_2(y_3 - 4) \quad (43)$$

Among them, $0 < y_1 < 0.25$, $0 < y_2 < 0.015$, $2 < y_3 < 6$.

Model 3 Multi-dimensional quality gain–loss calculation based on the Gaussian process

According to conditions 1, 2, and 3 in Table 4, the multi-dimensional quality gain–loss function based on the Gaussian process can be obtained as follows:

$$G(y(x)) = 0.320\left[384y_1(x)^2 - 2.4\right] + 0.123\left[106667y_2^2 - 640y_2\right] \\ +0.557\left[6(y_3 - 4)^2 - 3\right] \quad (44)$$

Ten groups of concrete mix samples were randomly selected, and the temperature recovery rate $y_1(x_i)$, mortar loss rate y_2, and silo surface collapse rate y_3 were recorded during transportation. The sample data records are shown in Table 5.

Table 5. Sample data records.

Group	1	2	3	4	5	6	7	8	9	10
y_1 (x_i)	0.12	0.18	0.22	0.1	0.15	0.18	0.11	0.17	0.18	0.2
y_2 (%)	0.01	0.005	0.009	0.014	0.005	0.006	0.01	0.01	0.005	0.011
y_3 (cm)	3	4	4.5	3.5	2.8	3.2	5	2.5	5.5	5.7

5.3.2. Comparative Analysis

The quality gain–loss values of each group of data can be obtained by substituting the sample data into three multi-dimensional quality gain–loss models. The quality gain–loss comparison table is shown in Table 6.

Table 6. Quality gain–loss comparison table.

Group	y_1 (x_i)	y_2 (%)	y_3 (cm)	Model 1	Model 2	Model 3
1	0.17	0.01	2.5	25.081996	16.672565	9.156532
2	0.15	0.005	2.8	28.948889	7.454505	5.072680
3	0.12	0.01	3	33.897795	5.545830	3.197272
4	0.18	0.006	3.2	40.527040	6.377674	3.681192
5	0.1	0.014	3.5	50.017889	3.652830	1.094740
6	0.18	0.005	4	64.083929	1.684948	1.476712
7	0.22	0.009	4.5	85.221640	9.682627	4.698132
8	0.11	0.01	5	99.107715	4.870369	2.914648
9	0.18	0.005	5.5	122.508928	14.358974	8.996212
10	0.2	0.011	5.7	130.610222	22.515333	11.753320

The data presented in the table demonstrate that the quality gain–loss value obtained from model 1 is greater than that from model 3 and model 2. Model 1 does not consider the correlation between quality features and the weight of each quality feature in the quality gain–loss, while models 2 and 3 consider both correlation and weight of quality characteristics. The comparison of quality gain–loss is shown in Figures 2 and 3.

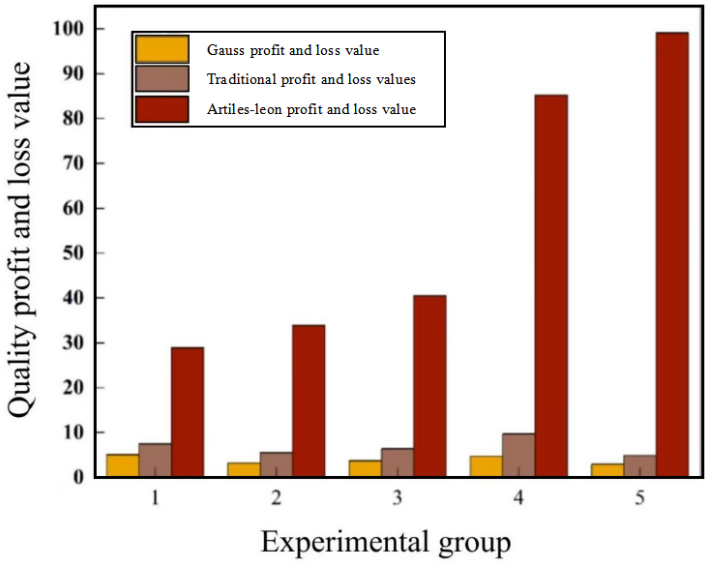


Figure 2. Quality gain–loss comparison chart.

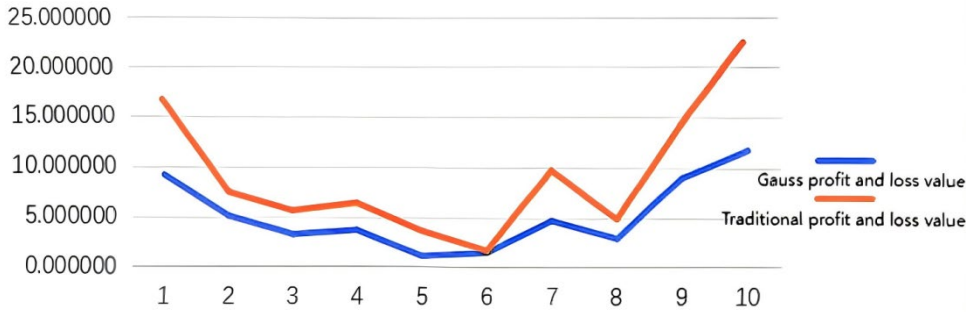


Figure 3. Quality gain–loss comparison chart (Gauss and traditional models).

As can be seen in Figure 2, the quality gain—-loss values of model 3 are all smaller than those of model 2. Model 3 not only considers the weight of each quality characteristic in the quality gain–loss but also considers the influence of multiple influencing factors on quality characteristics, so the calculation of quality gain–loss is more accurate. As shown in Figures 2 and 3, Model 1 exhibits significant errors in the calculated quality gain–loss values because it does not account for quality compensation or the weighting of quality characteristics. The traditional model incorporates quality compensation, and the comparison of gain–loss values demonstrates that its accuracy is more than 100% higher than that of the Artiles-León model. However, since the traditional model still neglects the weighting of different quality characteristics, certain errors remain in its results. In contrast, the proposed model not only considers quality compensation but also incorporates the influence of varying weights among quality characteristics, thereby improving accuracy by approximately 30% compared with the traditional model.

6. Conclusions

In the quality control of dam concrete construction during high-temperature seasons, this study considers temperature rise rate, mortar loss rate, and slump as the three primary quality characteristics. Placement speed, surface exposure time, and outlet temperature are identified as the influencing factors of the temperature rise rate. Based on the sample data of these factors, a Gaussian process regression model is established to obtain the experimental data of the temperature rise rate. Subsequently, a gain–loss cost matrix is derived using the signal-to-noise ratio, which is then employed to construct a multivariate and multidimensional quality gain–loss function model.

(1) By comparing the gain–loss values from the proposed function model with those obtained using the traditional multivariate quality gain–loss function and the dimensionless standardized multivariate function of Artiles-León, it is demonstrated that the proposed model exhibits clear advantages in addressing quality gain–loss problems under multiple quality characteristics and influencing factors.

(2) As an extension of the conventional quality gain–loss function, the multivariate and multidimensional quality gain–loss function, when integrated with the Gaussian process framework, not only accounts for interactions among multiple quality characteristics but also enables simultaneous evaluation of control effectiveness across different types of quality characteristics. This integration broadens the application scope of the quality gain–loss function in dam concrete construction quality control.

These findings provide both theoretical insights and practical implications for improving quality management in large-scale concrete projects, particularly under complex construction conditions.

Author Contributions: B.W.: conceptualization, methodology, formal analysis, writing—original draft; Q.L.: methodology, data curation; L.P.: visualization, investigation; P.L.: resources, supervision; H.L.: software, investigation; X.N.: visualization, writing—review and editing; T.F.: conceptualization, funding acquisition, resources. All authors have read and agreed to the published version of the manuscript.

Funding: This work was supported by the Research on Digitalization and Intelligentization-Driven Collaborative Governance in the Wen'anwa Flood Storage (2025-85) and Detention Zone Construction Project, Power CHINA Roadbridge Group Co., Ltd. (DJLQKJ2023), the Power Construction Corporation of China, Ltd. (DJKJ2023), and the Training Programme for Young Backbone Teachers of Higher Education Institutions in Henan Province (2024GGJS061).

Institutional Review Board Statement: Not applicable.

Data Availability Statement: The datasets generated or analyzed during this study are available from the corresponding author upon reasonable request.

Conflicts of Interest: Author Pengyuan Li was employed by the company Central China Regional Headquarters of Powerchina Road-Bridge Co., Ltd. The remaining authors declare that the research was conducted in the absence of any commercial or financial relationships that could be construed as a potential conflict of interest.

References

1. Gan, Y.F.; Li, Q.B.; Hu, Y. Dry curing strength and microstructure of concrete of Baihetan dam. *J. Hydroelectr. Eng.* **2022**, *41*, 42–49.
2. Fan, X.Q.; Liu, J.D.; Ge, F.; Tang, L.; Han, H. Comparative study on mechanical properties of concrete for a hydraulic complex project. *Hydro-Sci. Eng.* **2023**, *2*, 129–137.
3. Dong, Y.; Zhou, Z.C.; Li, P.X.; Liu, C. Long-term effectiveness of preventive measures against alkali-aggregate reaction of Jinping-I dam concrete. *J. Yangtze River Sci. Res. Inst.* **2022**, *39*, 140–144, 152.
4. Li, R.Q.; Pai, L.F.; Wu, H.G. Research and simulation of hydration heat of special-shaped mass concrete. *Sci. Technol. Eng.* **2021**, *21*, 10452–10460.
5. Lyu, G.E.; Tang, Q.Y.; Wang, D.S.; Li, T.; Zhu, Y.; Chen, D. Calculation method of heat damage by hydration of mass concrete. *J. Hohai Univ. (Nat. Sci.)* **2024**, *52*, 29–34.
6. Wang, X.G.; Peng, Y.F.; Yang, M.G. Research on hydration heat of mass concrete at arch support and temperature control measures for a high-speed railway tied-arch bridge. *J. Railw. Sci. Eng.* **2020**, *17*, 549–555.
7. Tasri, A.; Susilawati, A. Effect of cooling water temperature and space between cooling pipes of post-cooling system on temperature and thermal stress in mass concrete. *J. Build. Eng.* **2019**, *24*, 100731. [CrossRef]
8. El-Mir, A.; Assaad, J.J.; Nehme, S.G.; El-Hassan, H. Correlating strength and durability to time-temperature profiles of high-performance mass concrete. *Case Stud. Constr. Mater.* **2022**, *16*, e01055. [CrossRef]
9. Van Tran, M.; Chau, V.N.; Nguyen, P.H. Prediction and control of temperature rise of massive reinforced concrete transfer slab with embedded cooling pipe. *Case Stud. Constr. Mater.* **2023**, *18*, e01817. [CrossRef]

10. Qiao, Y.; Yang, N.; Tan, P.; Peng, H.; Wu, W.; Zhou, D.; Wang, X. Engineering application and factors affecting infrared temperature measurements of mass concrete surfaces. *J. Tsinghua Univ. (Sci. Technol.)* **2021**, *61*, 730–737.
11. Yang, N.; Liu, Y.; Qiao, Y.; Tan, Y.; Zhu, Z. Intelligent spray control for the concrete curing of mass concrete bins. *J. Tsinghua Univ. (Sci. Technol.)* **2021**, *61*, 724–729.
12. Deng, K.D.; Qiang, S.; Jiang, Y.B.; Xu, C.L. Research on unmanned transportation and pouring system model for hydraulic mass concrete construction. *Int. J. Hydroelectr. Energy* **2022**, *40*, 175–179.
13. Cui, W.; Liu, W.; Guo, R.; Wan, D.; Yu, X.; Ding, L.; Tao, Y. Geometrical quality inspection in 3D concrete printing using AI-assisted computer vision. *Mater. Struct.* **2025**, *58*, 68. [CrossRef]
14. Cui, W.; Ji, D.; Shen, L.; Su, S.; Shi, X.; Liu, J.; Bai, Z.; Sun, Y.; Gong, J.; Tao, Y. A neural network-based model for assessing 3D printable concrete performance in robotic fabrication. *Results Eng.* **2025**, *27*, 105970. [CrossRef]
15. Wang, B.; Li, Q.; Li, P.; Zhang, P.; Fan, T. Quality gain-loss transmission in dam concrete construction: A CF-GERT-based approach. *Int. J. Ind. Eng. Comput.* **2025**, *16*, 963–978. [CrossRef]
16. Cao, Y.-L.; Mao, J.; Yang, J.-X.; Wu, Z.-T.; Wu, L.-Q. Robust tolerance design based on fuzzy quality loss. *J. Zhejiang Univ. (Eng. Sci.)* **2004**, *38*, 1–4, 10. [CrossRef]
17. Wang, B.P.; Zhang, H.; Jing, D.Y. Study on section curve quality loss function model. *Trans. Chin. Soc. Agric. Mach.* **2007**, *38*, 150–152.
18. Zhao, Y.M.; Liu, D.S.; Zhang, J.; Liu, Q. Quality loss cost model and its application to products with multi-quality characteristics. *J. Cent. South Univ. (Sci. Technol.)* **2012**, *43*, 1753–1763.
19. Yang, C.M.; Duan, S.Q. Robust synthesis of function mechanisms by using asymmetric quality loss models. *J. Xihua Univ. (Nat. Sci.)* **2016**, *35*, 30–33.
20. Zeybek, M.; Köksoy, O. Optimization of correlated multi-response quality engineering by the upside-down normal loss function. *Eng. Optim.* **2016**, *48*, 1419–1431. [CrossRef]
21. Zhang, Y.Y.; Song, M.S.; Han, Z.J.; Chen, X.L. Design of quality loss function under the smaller the better characteristic without neglecting the linear term. *Ind. Eng. J.* **2011**, *14*, 81–83, 89.
22. Zhang, Y.Y.; Song, M.S.; Han, Z.J. Designing of the quality loss function of the larger the better characteristic under not neglecting the linear term. *J. Appl. Stat. Manag.* **2013**, *32*, 486–491.
23. Pignatiello, J.J. Strategies for robust multi-response quality engineering. *IIE Trans.* **1993**, *25*, 5–15. [CrossRef]
24. Artiles-León, N. A pragmatic approach to multiple-response problems using loss functions. *Qual. Eng.* **1996**, *9*, 213–220. [CrossRef]
25. Lee, C.L.; Tang, G.R. Tolerance design for products with correlated characteristics. *Mech. Mach. Theory* **2000**, *35*, 1675–1687. [CrossRef]
26. Ai, Y.T.; Tian, J.; Gao, H.C. Study on assembly quality optimization technology based on multivariate quality loss and genetic algorithm. *China Mech. Eng.* **2012**, *23*, 1161–1164.
27. Tansel, I.Y.; Yildirim, S. Moora-based Taguchi optimisation for improving product or process quality. *Int. J. Prod. Res.* **2013**, *51*, 3321–3341. [CrossRef]
28. Wu, J.J.; Xie, Z.W.; Huang, Y.L. A new method for multi-response robust optimization based on improved quality loss function. *Mech. Sci. Technol. Aerosp. Eng.* **2017**, *36*, 519–526.
29. Zhong, H.M.; Wu, H.C. Multi-response robust design based on comprehensive weight and quality loss. *Mech. Sci. Technol. Aerosp. Eng.* **2017**, *36*, 903–908.
30. Wang, B.; Fan, T.Y.; Tian, J. Designing a quality gain-loss function for larger-the-better characteristic and smaller-the-better characteristic under not neglecting the linear term loss and keeping compensation amount constant. *Math. Pract. Theory* **2019**, *49*, 153–160.
31. Wang, B.; Zhou, H.G.; Li, Z.Y.; Nie, X.T. Tolerance optimization for quality characteristics of the dam concrete construction based on quality gain-loss function. *Math. Pract. Theory* **2016**, *46*, 90–99.
32. Wang, B.; Li, Q.; Liu, C.; Chen, Z.; Nie, X. Establishment and application of a grey quality gain–loss function model. *Processes* **2022**, *10*, 495. [CrossRef]
33. Wang, B.; Li, Q.; Yang, Q.; Lu, J.; Nie, X. Improvement of quadratic exponential quality gain–loss function and optimization of engineering specifications. *Processes* **2023**, *11*, 2225. [CrossRef]
34. Wang, B.; Zhou, H.; Li, Z.; Fan, T.; Nie, X. Quality gain-loss function and its empirical analysis in dam concrete construction. *J. Coast. Res.* **2020**, *104*, 842–848. [CrossRef]
35. Wang, B.; Li, X.; Shi, J.; Li, Q.; Nie, X. The establishment and application of quality gain-loss function when the loss of primary and cubic term is not ignored and the compensation quantity is constant. *PLoS ONE* **2023**, *18*, e295949. [CrossRef]
36. Zhang, Y.; Su, G.S.; Yan, L.B. Strength prediction of high strength concrete using Gaussian process machine learning. *Concrete* **2011**, *11*, 18–20.
37. Luo, Y.Y. A Gaussian process based model for predicting deformations of dams. *J. Zhejiang Univ. Technol.* **2016**, *44*, 543–546.

38. Zhai, C.H.; Wang, J.J.; Feng, Z.B. Robust parameter design of multiple responses based on Gaussian process model. *Syst. Eng. Electron.* **2021**, *43*, 3683–3693.
39. Liu, M.H.; Wang, X.L.; Wang, J.J. Study on improved multi-output prediction model for compaction characteristics of earth-rock dam materials. *J. Hydroelectr. Eng.* **2022**, *41*, 63–73.
40. Ma, J.T.; Kang, F.; Jiang, C.L.; Xiang, Z.L.; Wang, Y.F. Jaya-Gaussian process regression model for parameter inversion of high arch dams. *Adv. Sci. Technol. Water Resour.* **2022**, *42*, 74–79.
41. Mao, Y.X.; Zhang, Y.; Jia, B.J. Application research of medium and long term runoff forecast of hydropower station based on data mining. In Proceedings of the China Hydropower Engineering Society Automation Committee 2022 Annual Meeting and the National Hydropower Plant Intelligent Application Academic Exchange Meeting, Nanjing, China, 7–9 August 2022.
42. Huang, L.; Chen, S.; Li, C.; Si, Z.; Zhang, F. Application of Gaussian process regression model based on wavelet denoising in settlement prediction of CFRD. *J. Water Resour. Water Eng.* **2023**, *34*, 144–150.
43. Liu, W.Q.; Chen, B. Prediction model of dam deformation driven by NGO-GPR and projection pursuit. *J. Hydroelectr. Eng.* **2023**, *42*, 126–136.
44. Li, H.K.; Ke, X.Y.; Huang, W.; Liu, S.P.; Tang, Y.Y. Inversion study of soft foundation sluice bottom plate emptying based on a GPR surrogate model and a GA-APSO hybrid optimization algorithm. *J. Vib. Shock* **2023**, *42*, 1–10.
45. Li, W.H.; Lou, J.K.; Li, X. Combined kernel function-based gaussian process dam deformation prediction method. *Yelloe River* **2023**, *45*, 137–140.
46. Chen, X.H.; Hu, Y.; Wang, Y.J.; Zhu, X.Z. Dam deformation interval prediction model based on XGBoost. *J. Hydroelectr. Eng.* **2024**, *43*, 121–136.

Disclaimer/Publisher's Note: The statements, opinions and data contained in all publications are solely those of the individual author(s) and contributor(s) and not of MDPI and/or the editor(s). MDPI and/or the editor(s) disclaim responsibility for any injury to people or property resulting from any ideas, methods, instructions or products referred to in the content.